Efficiency of plasma actuator ionization in shock wave modification in a rarefied supersonic flow over a flat plate

Romain Joussot*, Viviana Lago* and Jean-Denis Parisse†

*ICARE, CNRS, UPR 3021, 1C Avenue de la Recherche Scientifique, 45071, Orléans Cedex 2, France
†IUSTI, Aix Marseille Université / CNRS, UMR 7343, 5 rue Enrico Fermi, Technopôle Château-Gombert, 13453, Marseille Cedex 13, France

Abstract. This paper describes experimental and numerical investigations focused on the shock wave modification, induced by a dc glow discharge, of a Mach 2 flow under rarefied regime. The model under investigation is a flat plate equipped with a plasma actuator composed of two electrodes. The glow discharge is generated by applying a negative potential to the upstream electrode, enabling the creation of a weakly ionized plasma. The natural flow (i.e. without the plasma) exhibits a thick laminar boundary layer and a shock wave with a hyperbolic shape. Images of the flow obtained with an ICCD camera revealed that the plasma discharge induces an increase in the shock wave angle. Thermal effects (volumetric, and at the surface) and plasma effects (ionization, and thermal non-equilibrium) are the most relevant processes explaining the observed modifications. The effect induced by the heating of the flat plate surface is studied experimentally by replacing the upstream electrode by a heating element, and numerically by modifying the thermal boundary condition of the model surface. The results show that for a similar temperature distribution over the plate surface, modifications induced by the heating element are lower than those produced by the plasma. This difference shows that other effects than purely thermal effects are involved with the plasma actuator. Measurements of the electron density with a Langmuir probe highlight the fact that the ionization degree plays an important role into the modification of the flow. The gas properties, especially the isentropic exponent, are indeed modified by the plasma above the actuator and upstream the flat plate. This leads to a local modification of the flow conditions, inducing an increase in the shock wave angle.

Keywords: plasma devices; supersonic flows; flow control; glow discharge; shock wave; ionization; rarefied gas dynamics
PACS: 52.75.-d; 47.40.Ki; 47.85.L-; 52.80.Hc; 47.40.Nm; 52.25.Jm; 47.45.-n

INTRODUCTION

Flow control (active or passive methods) research in compressible regime plays a major role in aerospace and transportation applications. Passive flow control methods are simple and economic because they do not require any power input or loop control. However, the most drawback of such system is that they are optimized for only one aerodynamic configuration. Active flow control methods have therefore been developed to be used for several aerodynamic configurations. Active methods using plasma devices have increased in importance over the last few years [1, 2]. Compared to traditional active flow control methods, active plasma actuators present several advantages like a fast-time response, their low weight and size and the relatively low energy consumption, offering promising applications for flight control systems at high velocities [1, 3, 4, 5, 6, 7, 8, 9, 10, 11]. Other examples of plasma flow application concern the change in the trajectory of a flying vehicle. The application concerns guided anti-aerial projectiles in which a short plasma discharge is used to deviate the projectile from the initial trajectory. In this case the plasma discharge replaces the commonly pyrotechnical systems working only once [12]. Under supersonic flow conditions, Joule heating is commonly interpreted as the main physical mechanisms responsible of aerodynamics effects, resulting from electrical discharges created in air flow [4, 7, 13]. A number of experimental works have been undertaken at high speed flows [4, 7]. Nevertheless it still remains experiments which can be hardly explained by thermal effects. In such cases, the quantification of the non-thermal mechanisms is very important for future applications and meanwhile very difficult to overcome because they act in addition to thermal effects like the gas heating and the Joule heating which can overshadow non-thermal effects [14, 15, 16]. Many types of plasma actuator are developed and could be more or less efficient regarding the flow regime conditions, it may be mentioned, thermal arcs, dielectric barrier discharges or glow discharges. Non equilibrium glow discharges are particularly attractive compared to thermal arcs because they have low power requirements and a wide field of flow actuation taking place through volumetric heating, heating of solid surfaces, and electrostatic forces. This work follows in the footstep of earlier studies concerning the interaction of a glow discharge and a shock wave formed above a flat plate with a Mach

2 rarefied flow [9, 17]. This paper presents a joined effort between numerical simulation and experiments in order to have a better understanding of the phenomena involved. New experiments revealed the role played by the ionization rate of the plasma actuator on the shock wave modification which supplements the thermal effects already mentioned [9, 17]. The evidence of the thermal nature of the interaction is overwhelming. However, the present work presents a significant improvement because the temperature gradient over the flat plate is taken into account on the numerical description of the thermal effects.

EXPERIMENTAL SET-UP

The MARHy wind tunnel

The MARHy low density facility (formerly known as SR3, Lab. Aérothermique, see [18] for further details) is used both for academic and industrial researches. In this low density facility (diameter of 1.3 m, length of 5 m), an adapted nozzle provides a stationary flow with Mach numbers ranging between 0.8 and 20 in continuous operating mode. The pumping system is composed of 2 primary pumps, 2 intermediary Roots blowers and 12 Roots blowers. The nominal operating conditions of this work are summarized in table 1.

TABLE 1. Operating conditions

Stagnation conditions	**Flow conditions**
$p_{st} = 63\,\mathrm{Pa}$	$p_0 = 8\,\mathrm{Pa}$
$T_{st} = 300\,\mathrm{K}$	$T_0 = 163\,\mathrm{K}$
$\rho_{st} = 7.44 \times 10^{-4}\,\mathrm{kg{\cdot}m^{-3}}$	$\rho_0 = 1.71 \times 10^{-4}\,\mathrm{kg{\cdot}m^{-3}}$
	$\mu_0 = 1.10 \times 10^{-5}\,\mathrm{Pa{\cdot}s}$
	$v_0 = 511\,\mathrm{m{\cdot}s^{-1}}$
	$M_0 = 2$
	$\lambda_0 = 0.375\,\mathrm{mm}$
	$q_m = 3.34 \times 10^{-3}\,\mathrm{kg{\cdot}s^{-1}}$

Diagnostics

The operating wind tunnel parameters (stagnation pressure, test section pressure) are continuously measured with absolute pressure transducers. The flow field pressure profiles above the plate are obtained with a Pitot probe made of glass in order to avoid electrical interactions with the discharge. The Pitot tube is a flat-ended cylinder with an external diameter of $D = 6\,\mathrm{mm}$ and an internal diameter of $d = 4\,\mathrm{mm}$. The probe is connected to a pressure transducer (0-1 Torr). A 3-axis traversing system, controlled by a computer, ensures the translation of the Pitot probe with a step resolution on each axis of $0.1\,\mathrm{mm} \pm 0.02\,\mathrm{mm}$ on each position. The flow around the flat plate is imaged by a PI-MAX Gen-II ICCD camera ($1024 \times 1024\,\mathrm{pixels}$) equipped with a VUV objective lens (94 mm and $f/4.1$). The light is collected through a quartz window located in the wall of the test section chamber (see [19] for further details on the optical arrangement). An infrared thermography device is used to measure the flat plate temperature distribution during experiments with the plasma actuator and the heater actuator. The IR camera FLIR ThermaCAM SC 3000 is placed on the top of the wind tunnel and focuses the entire surface of the flat plate through a fluorine window compatible with IR wavelength range. The camera is equipped with an IR photo-detector of QWIP type constituted of $320 \times 240\,\mathrm{pixels}$, working in the wavelength region between 8 and 9 µm. As the metallic electrodes act as a body with no intrinsic emissivity, two longitudinal thin black lines are painted on the surface of the flat plate. The emissivity is estimated to be $\varepsilon = 0.96$. For each electrical condition tested (with the plasma actuator or with the heater), the temperature measurements were acquired after waiting that the thermal equilibrium was achieved ($\approx 10 - 20\,\mathrm{min}$). Each thermogram was obtained by averaging 100 images recorded at 1 Hz. A Langmuir probe was used to measure the electron density and temperature of the flow modified by the plasma actuator in order to estimate the local ionization rate [20]. The technique used is that of single plane probe made with a tungsten wire of circular section (1 mm in diameter) insulated within an alumina tube of 3 mm in external diameter. The probe is mounted vertically on the 3-axis traversing system and is connected to a voltage generator delivering periodic triangular signals with adjustable rise and fall times.

Flat plate and actuators

The model under investigation is a flat plate (100 mm long, 80 mm wide, and 4 mm thick) made of quartz with a sharp leading edge (15°), mounted 174 mm downstream the nozzle exit (see figure 1). Considering the experimental conditions (table 1) and the flat plate length, the Reynolds number is 794 and the Knudsen number is 4×10^{-3} .

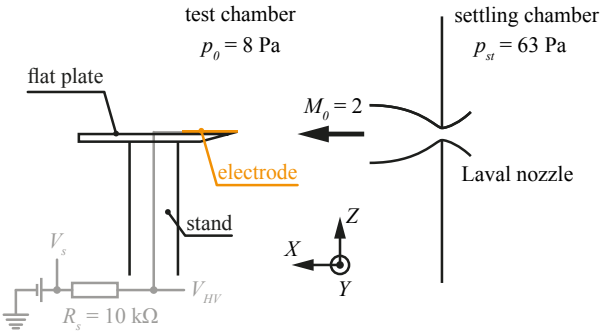

FIGURE 1. Schematic view of the flat plate.

Two types of actuator have been investigated to discriminate the role of the thermal effects involved in plasma actuator with respect to other effects produced by the plasma discharge like ionization. The plasma actuator is composed of two aluminum electrodes (80 mm long and 35 mm wide) with a thickness of 80 µm, which are flush mounted on the upper surface of the flat plate (see figure 2*(a)*). The active electrode is set at the leading edge of the plate and is connected to a high voltage dc power supply (Spellman SR15PN6) through a resistor ($R_s = 10.6\,\text{k}\Omega$), while the second one is grounded. The glow discharge is generated by applying a negative dc potential to the active electrode, acting as a cathode. The voltage V_s is fixed with the power supply, which delivers the discharge current I_{HV}. The voltage applied to the electrode V_{HV} is then calculated with the following relation: $V_{HV} = V_s - R_s \cdot I_{HV}$. The discharge is ignited in air at $V_{ign} = -0.38\,\text{kV}$, and can be sustained down to around $V_{HV} \approx -2.5\,\text{kV}$. Within this range the discharge current I_{HV} increases linearly with the applied voltage V_{HV}. This behavior corresponds to the abnormal glow discharge regime [21]. The electrical characteristics of the glow discharge are presented in figure 3.

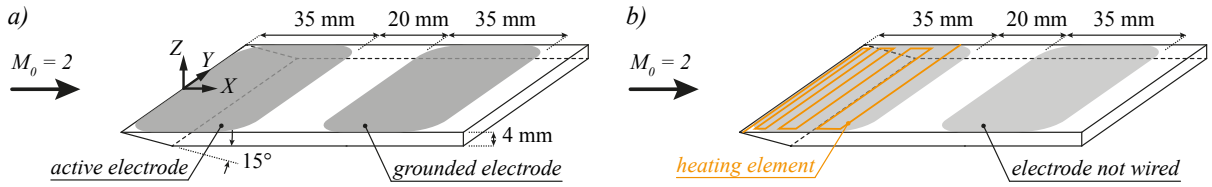

FIGURE 2. Schematic views of the flat plate with: *(a)* the plasma actuator and *(b)* the heating element.

Previous works [9, 17, 22] have shown that one of the discharge plasma effects is the heating of the plate surface. The surface heating is due, first to an ohmic heating, and second to the electrode bombardment by ions and neutrals from the plasma to the wall relied on the electric field in the vicinity of the cathode. This last point influences the surface temperature distribution along the longitudinal X-direction, which is evidenced by the infra-red camera measurements presented in figure 4*(a)*. To reproduce only the thermal effect at the wall induced by the plasma actuator, an actuator composed of a heating element (called the heater) is manufactured. It is composed of a 0.15 mm-diameter Constantan wire ($28\,\Omega{\cdot}\text{m}^{-1}$) embedded between two layers of polyimide film. The heater is flush mounted on the flat plate surface instead of the cathode as presented on figure 2*(b)*. In order to preserve the same flow topology than those of the plasma actuator, the grounded electrode is present on the surface plate but not wired. The longitudinal distribution of the wire is not homogeneous in order to reproduce the temperature distribution measured with the discharge (figure 4*(b)*). The heater is supplied by a continuous power supply ($0-60\,\text{V}$, $0-2.5\,\text{A}$).

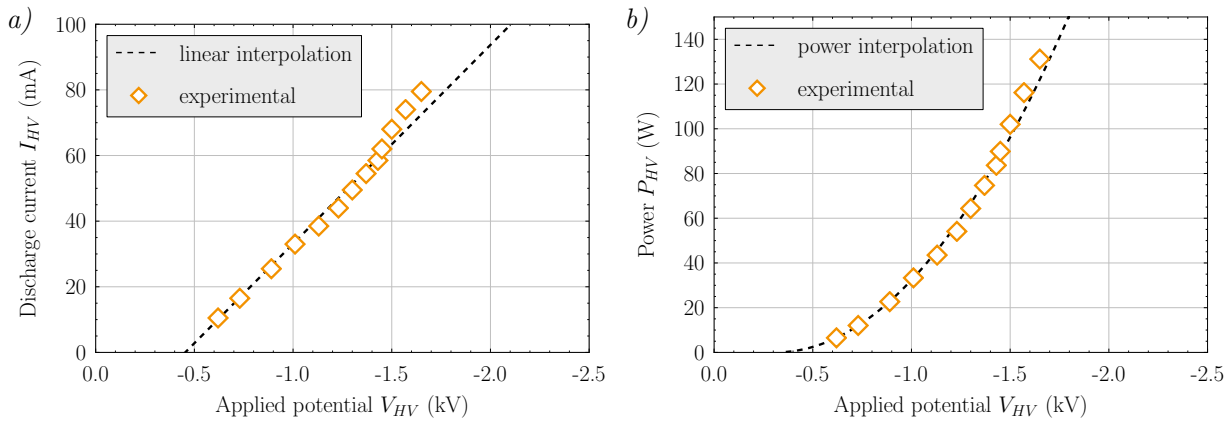

FIGURE 3. Electrical characterization of the discharge in a Mach 2 air flow: *(a)* current-voltage characteristic and *(b)* power consumption versus the applied voltage.

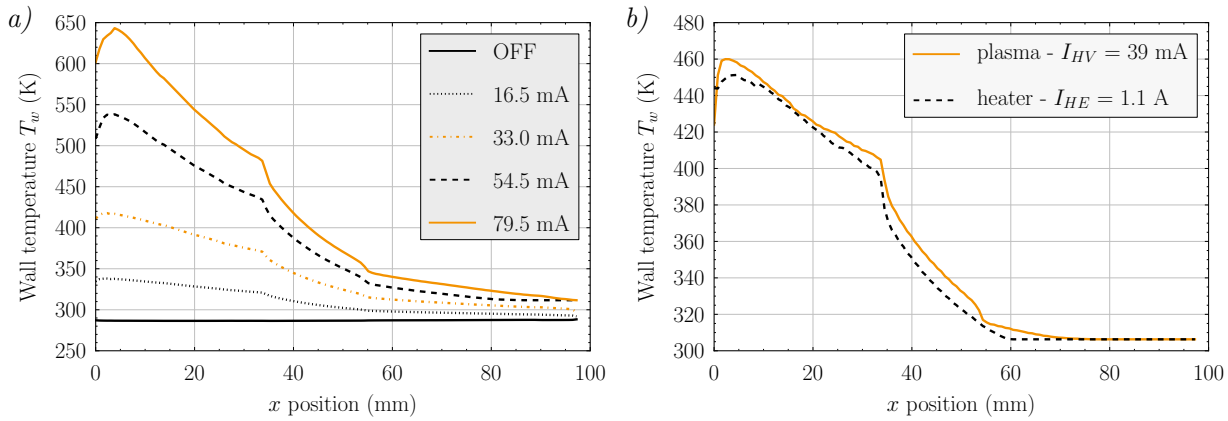

FIGURE 4. Distribution of the surface temperature T_w along the flat plate: *(a)* with the plasma actuator and *(b)* comparison of T_w between the plasma actuator ($I_{HV} = 39\,\text{mA}$) and the heating element ($I_{HE} = 1.1\,\text{A}$). The free stream Mach number is 2.

THE BASELINE FLOW

The flow field around the flat plate is investigated without any actuator, namely the natural flow case. The shock wave is experimentally visualized with the glow-discharge flow visualization technique. Figure 5*(a)* shows the natural flow around the flat plate visualized with the ICCD camera where the shock wave is readily recognized, enabling the estimation of its shape. Each image obtained with the ICCD camera results from the averaging and post-processing of 300 images in order to distinguish the shock wave position more precisely than is possible from a raw image. The contrast is enhanced with ImageJ software. In our conditions, the shape of the natural shock wave is hyperbolic and the shock wave angle β is estimated from the angle of the hyperbola asymptote (figure 5*(b)*). In our experimental conditions, β is estimated to be 36.4°. The natural Mach 2 flow field is simulated with a WENO code, consisting in a Navier-Stokes code with adapted slip conditions to simulate rarefied flow regimes [19]. Simulations are run with the input parameters corresponding to the experimental flow conditions (table 1). The resulting Mach number flow field is shown in figure 5*(c)*. The global shape of the shock wave is well reproduced and the calculated value of the shock angle is 37.5°, which is slightly larger than the experimental value. Moreover, the simulation confirms that the shock wave is detached. The natural flow field above the flat plate was mapped by means of the Pitot probe. Figure 6 shows the total pressure profiles, namely the Pitot pressure, for several longitudinal positions along the flat plate. The number of wall-normal positions recorded for pressure profiles was gradually increased while the boundary layer thickened. The dashed lines represent the Pitot pressure extracted from the simulated flow field. One can observe that the overall

shape of each pressure profile is well reproduced. The fact that the simulation slightly overestimates the shock wave angle can be relied on the development of the boundary layer along the flat plate. The boundary layer thickness of the numerical flow field is indeed higher than those estimated with the experimental data.

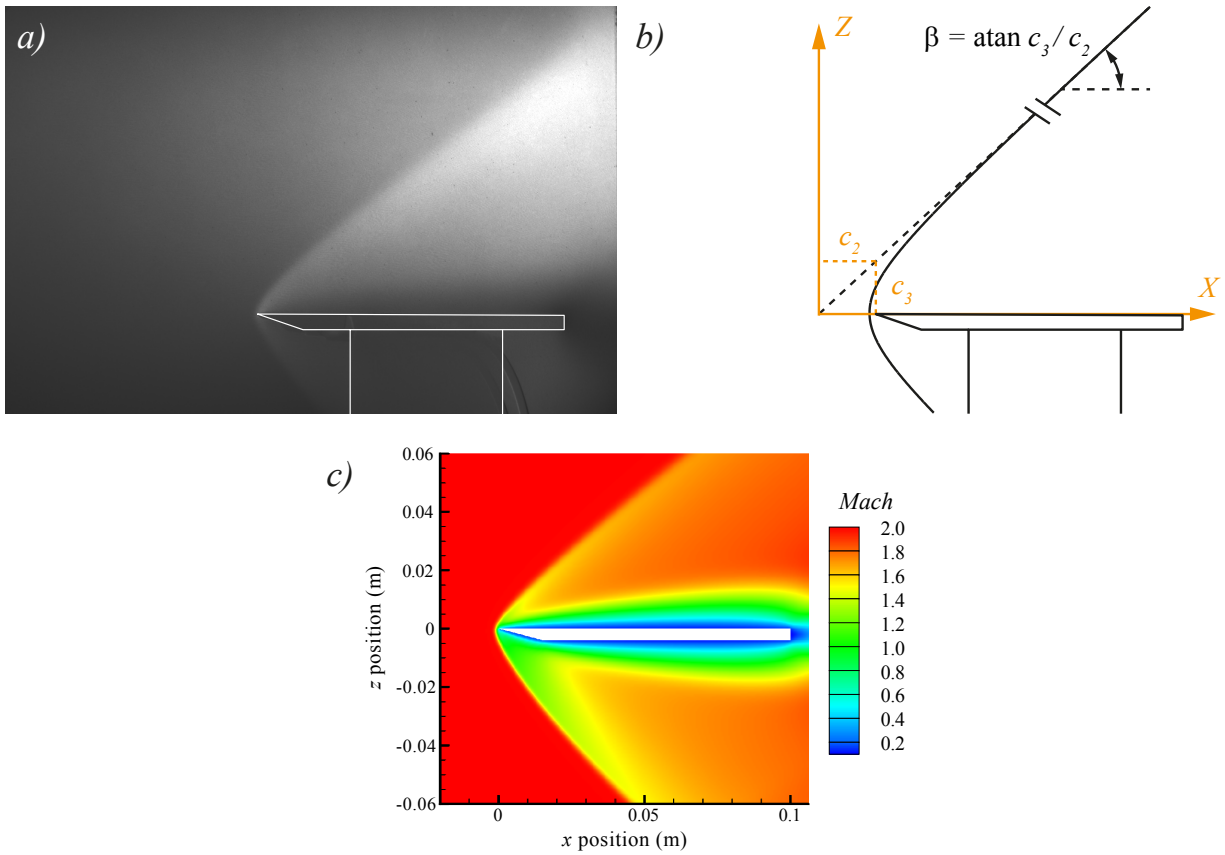

FIGURE 5. Image of the natural flow field around the flat plate obtained with the glow-discharge flow visualization technique *(a)*, schematic view of the shock-wave shape and the corresponding shock wave angle β, and *(c)* Mach number flow field from the WENO simulation of the natural flow. The free stream Mach number is 2.

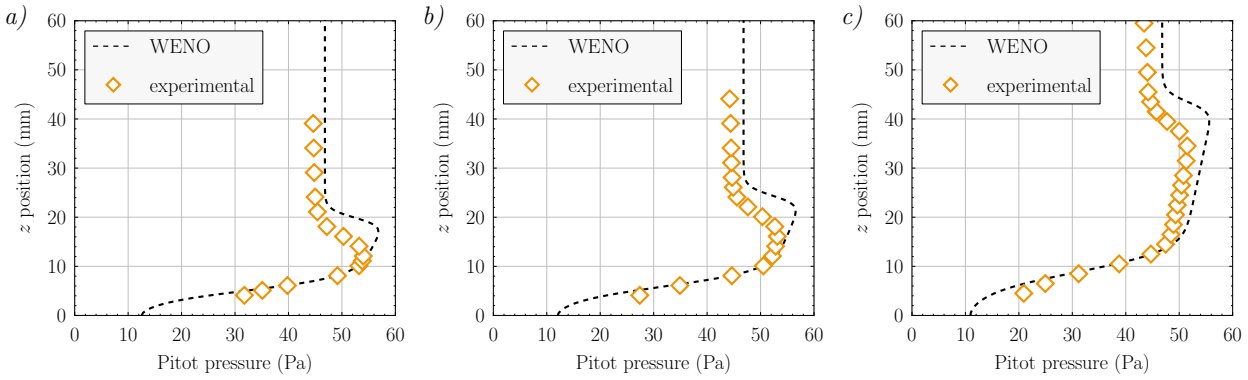

FIGURE 6. Pressure profile without actuation at: *(a)* $x = 17.5$ mm, *(b)* $x = 22.5$ mm, and *(c)* $x = 45.0$ mm. The free stream Mach number is 2.

ANALYSIS OF THE SHOCK WAVE ANGLE INCREASE

When the discharge is switched on, the shock wave is deflected outward the flat plate surface as illustrated in figure 7*(a)*, where the natural shock wave shape (solid line) is superimposed on the image in order to facilitate the comparison. The dark area above the cathode corresponds to the plasma sheath. The shock wave angle is determined for each discharge operating condition tested. Figure 7*(b)* shows the variation of the shock angle with the current discharge, illustrating that higher is the discharge current, higher is the increase in the shock wave angle.

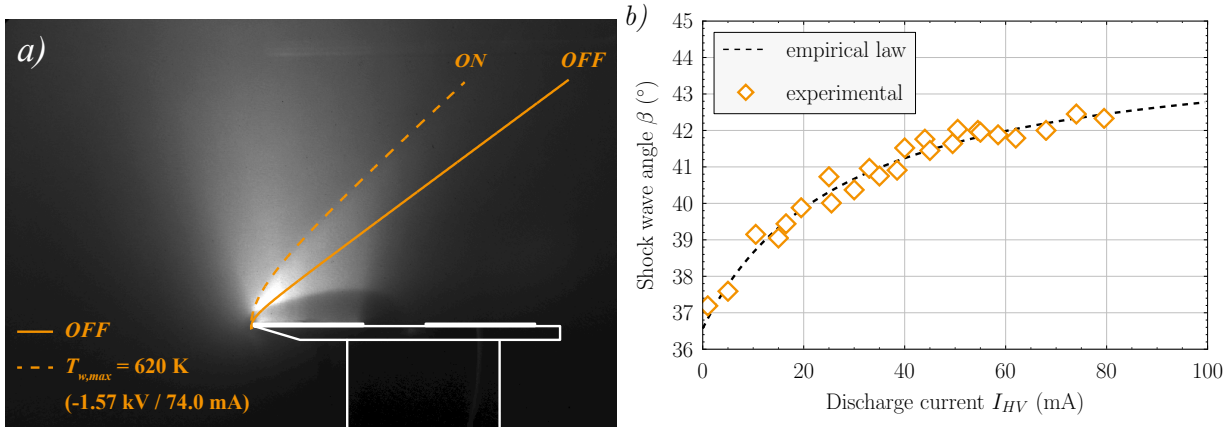

FIGURE 7. Modification of the shock wave by the plasma actuator: *(a)* ICCD image of the flow modified by the discharge ($V_{HV} = -1.57\,\text{kV}$ and $I_{HV} = 74\,\text{mA}$), the solid line represents the shock wave shape of the baseline, and *(b)* shock wave angle β according to the discharge current I_{HV}. The free stream Mach number is 2.

To evaluate the surface thermal effects on the flow field modifications, experiments have been carried out using the heater as actuator. The analysis of the ICCD images shows that the surface heating induced with the heater produces an increase in β (figure 8, black triangles). However, for a same wall temperature, the shock angle values are lower than those obtained with the plasma actuator (figure 8, orange diamonds). When the heater is used, one can reasonably think that only a purely-thermal effect can explain the flow modification. In this case, the mechanisms involved are linked to the modification of the flow viscosity above the heater, leading to a thickening of the laminar boundary layer and hence an increase in β. The numerical simulations obtained with different wall temperature distributions give similar results (figure 8, purple circles). The results of figure 8 show that the Joule heating of the flat plate surface accounts for almost half of the total shock wave modification, illustrating clearly the fact that others mechanisms than the thermal one are involved in the shock wave modification by the plasma actuator.

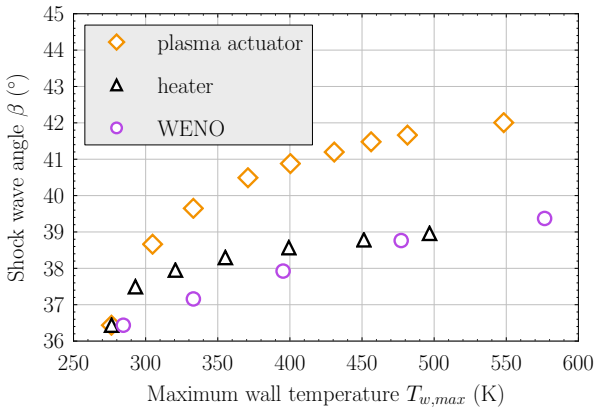

FIGURE 8. Comparison of the shock wave angles measured with the two types of actuator (plasma actuator: orange diamonds; heater: black triangles) and calculated with the numerical simulation (purple circles). The free stream Mach number is 2.

THE ROLE OF THE IONIZATION RATE ON THE SHOCK WAVE MODIFICATION

It is clear that the plasma actuator modifies the flow field in another way than via a thermal effect at the electrode surface. In addition, previous studies [9, 23] have shown that the volumetric heating is rather low (+10 K for a plasma discharge with a power ranged between 30 W and 90 W), meaning that other effects induced by the discharge must be studied to explain the shock wave modification observed. In [19], the authors have shown that a Mach 2 flow field around a cylinder is modified by a plasma actuator applied over the cylinder surface because the ionization rate is strong enough to decrease the value of the isentropic coefficient of the gas γ, leading to an increase in the stand-off distance. Although the nature of the shock wave is different (weak shock wave in this study, strong one in [19]), the conclusions drawn in [19] lead us to believe that the ionization rate could play a key role to explain the observed modifications over the flat plate, since the flow conditions are the same and the plasma actuator devices are similar. Measurements of the plasma properties (T_e and n_e) have therefore been achieved with a Langmuir probe in order to estimate the ionization rate induced by the discharge, in the vicinity of the cathode. A survey of the region upstream the flat plate was performed, since we think that the shock wave is modified by the upstream flow conditions. Figure 9*(a)* shows the vertical profile of electron density, at a longitudinal position of $x = -5$ mm for a plasma discharge with 30 mA and -1.13 kV. It may be note that the electron density profile presents a maximum at $z = 10$ mm, illustrating the fact that the discharge placed downstream the shock wave modifies the flow upstream the leading edge of the flat plate through the electrons for which the mobility obeys to the electric field configuration and not to the density field of the heavy particles. The electron density values are ranged between 8.8×10^{11} cm^{-3} and 1.5×10^{12} cm^{-3} and the electron temperature between 1.3 eV and 3.0 eV (not shown here), showing the strong non-thermal equilibrium state of the flow. In a diatomic plasma with non-local thermodynamic equilibrium, the isentropic exponent value depends on the ionization rate and on the thermal disequilibrium degree [24, 25]. According to [24, 25] and our measurements, the isentropic exponent of the gas in the discharge region is modified. Figure 9*(b)* shows the variation of the electron density according to the discharge current and the corresponding ionization rate, at $x = -5$ mm and $z = 10$ mm. These values lead to isentropic coefficient value ranged between 1.0×10^{-5} and 2.5×10^{-4} , meaning that the local decrease of γ upstream the shock wave has a direct influence on the interaction between the flat plate and the supersonic gas flow.

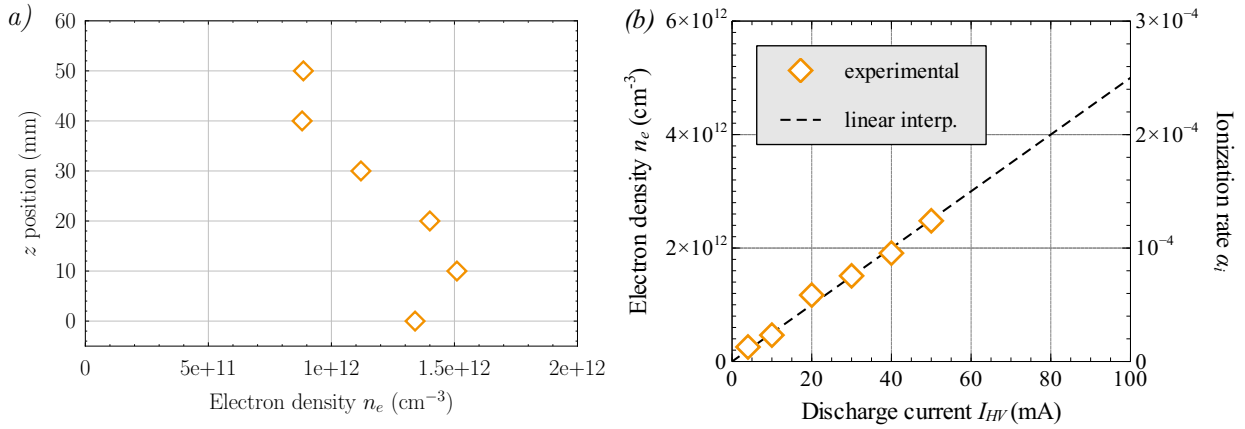

FIGURE 9. Variation of electron density n_e: *(a)* vertical distribution upstream the flat plate at $x = -5$ mm ($I_{HV} = 30$ mA and $V_{HV} = -1.13$ kV), and *(b)* evolution of n_e and the corresponding ionization rate α_i according to the discharge current I_{HV} at $x = -5$ mm and $z = 10$ mm. The free stream Mach number is 2.

CONCLUSIONS

This work focuses on the identification of significant effects of a plasma actuator acting over a weak shock wave on rarefied regime. It was experimentally observed that the increase in the discharge current of the plasma actuator induces an increase in the shock wave angle. In order to differentiate the thermal effects from a purely plasma effect, measurements with a heater actuator were carried out to estimate the thermal influence on the flow field modification. In addition, numerical simulations were carried out with a Navier-Stokes code modified with slip boundary conditions adapted to rarefied regime. The heating distribution along the plate is simulated numerically, reproducing the flow

modifications in the same way that those observed experimentally. This work demonstrates that the surface heating of the flat plate is responsible of approximately 50% of the shock wave angle increase, meaning that a purely plasma effect is responsible of the remaining part of the flow modification. To improve the understanding of how the plasma actuator acts, Langmuir probe measurements were done to estimate the electron properties (density and temperature). These measurements show that the ionization rate is strong enough to modify the gas properties, influencing the speed of sound and the Mach number in the region upstream the flat plate. This result lets us think that the modification of the flow properties by the plasma discharge, via the ionization rate, is one of the main mechanisms involved in the shock wave angle increase. Future experiments will be conducted to analyze the behavior of the electron density and temperature across the shock wave. These measurements will be coupled with optical spectroscopy measurements to investigate the thermal disequilibrium properties which could have an influence on shock wave modification. In addition, the numerical simulations will provide information about aerodynamic forces, like drag and lift efforts around the body, and their evolution with the electrical parameter of the plasma actuator.

ACKNOWLEDGMENTS

Romain Joussot's fellowship is provided by the French Government's Investissement d'Avenir program: Laboratoire d'Excellence CAPRYSSES (grant no. ANR-11-LABX-0006-01). Additional funding is provided by the Région Centre with the PASS grant (convention no. 00078782). The authors would like to acknowledge Dr. Ivan FEDIOUN for fruitful discussions.

REFERENCES

1. E. Moreau, *J. Phys. D: Appl. Phys.* **40**, R605–36 (2007).
2. L. Wang, Z. B. Luo, Z. X. Xia, B. Liu, and X. Deng, *Sci. China Tech. Sci.* **55**, 2225–40 (2012).
3. A. Klimov, V. Bityurin, and Y. Serov, "Non-thermal approach in plasma aerodynamics," in *AIAA Paper No. 2001-0348*, 2001.
4. V. E. Semenov, V. G. Bondarenko, V. B. Gildenburg, V. M. Gubchenko, and A. I. Smirnov, *Plasma Phys. Contr. F.* **44**, B293–B305 (2002).
5. V. M. Fomin, P. K. Tretyakov, and J.-P. Taran, *Aerosp. Sci. Technol.* **8**, 411–21 (2004).
6. V. A. Bityurin, and A. I. Klimov, "Non-thermal plasma aerodynamics effects," in *AIAA Paper No. 2005–978*, 2005.
7. P. Bletzinger, B. N. Ganguly, D. van Wie, and A. Garscadden, *J. Phys. D: Appl. Phys.* **38**, R33–R57 (2005).
8. S. B. Leonov, D. A. Yarantsev, V. G. Gromov, and A. P. Kuriachy, "Mechanisms of flow control by near-surface electrical discharge generation," in *AIAA Paper No. 2005–780*, 2005.
9. E. Menier, L. Leger, E. Depussay, V. Lago, and G. Artana, *J. Phys. D: Appl. Phys.* **40**, 695–701 (2007).
10. J. Shin, V. Narayanaswamy, L. Raja, and N. T. Clemens, "Characteristics of a plasma actuator in Mach 3 flow," in *AIAA Paper No. 2007–788*, 2007.
11. J. Shin, V. Narayanaswamy, L. Raja, and N. T. Clemens, *AIAA J.* **45**, 1596–605 (2007).
12. P. Gnemmi, and C. Rey, "Experimental and numerical investigations of a transverse jet interaction on a missile body," in *AIAA Paper No. 2005–0052*, 2005.
13. J. Menart, J. Shang, C. Atzbach, S. Magoteaux, M. Slagel, and B. Bilheimer, "Total drag and lift measurements in a Mach 5 flow affected by a plasma discharge and a magnetic field," in *AIAA Paper No. 2005–947*, 2005.
14. S. O. Macheret, M. N. Shneider, and R. B. Miles, *AIAA J.* **42**, 1378–87 (2004).
15. J. S. Shang, R. L. Kimmel, J. Menart, and S. T. Surzhikov, *J. Propul. Power* **24**, 923–34 (2008).
16. J. S. Shang, *J. Spacecraft Rockets* **45**, 1213–22 (2008).
17. J.-D. Parisse, L. Léger, E. Depussay, V. Lago, and Y. Burtschell, *Phys. Fluids* **21**, 106103 (2009).
18. J. Allegre, "The SR3 low density wind-tunnel. Facility capabilities and research development," in *AIAA Paper No. 92-3972*, 1992.
19. V. Lago, R. Joussot, and J. D. Parisse, *J. Phys. D: Appl. Phys.* **47**, 125202 (2014).
20. I. Langmuir, *The collected works of Irving Langmuir: Cloud nucleation*, vol. 11, Published with the editorial assistance of the General Electric by Pergamon Press, 1962.
21. Y. P. Raizer, *Gas discharge Physics*, Springer-Verlag, Berlin Heidelberg, 1991.
22. L. Leger, and E. Depussay, *Exp. Fluids* **53**, 699–706 (2012).
23. L. Léger, E. Depussay, and V. Lago, *IEEE T. Dielect. El. In.* **16**, 396–403 (2009).
24. K. T. A. L. Burm, W. J. Goedheer, and D. C. Schram, *Phys. Plasmas* **6**, 2622–7 (1999).
25. K. T. A. L. Burm, W. J. Goedheer, and D. C. Schram, *Phys. Plasmas* **6**, 2628–35 (1999).